

AD-A103 180 FLOW RESEARCH CO KENT WA
ARCTIC MECHANICAL ENERGY BUDGET. (U)
DEC 80 J J KOLLE
UNCLASSIFIED FLOW-RR-178

F/G 8/12

N00014-79-C-0147

NI

1 OF 1
AP-A
C-140

END
DATE
9-81
DTIC

LEVEL II



FLOW RESEARCH COMPANY

A DIVISION OF FLOW INDUSTRIES, INC.

ADA103180

FILE COPY



HEADQUARTERS
21414 - 68th Avenue South
Kent, Washington 98031 (206) 872-8500
Seattle Ex. 622-1500 TWX 910-447-2782

DTIC
ELECTE
S D
AUG 24 1981
D

DISTRIBUTION STATEMENT A
Approved for public release
Distribution Unlimited

81 7 17 083

Accession For	
NTIS	SP&L
DTIC	SPB
Unannounced	
Justification	
By <i>Per Lk. on file</i>	
Distribution/	
Availability Codes	
Aerial and/or	
DIST	Special
A	

LEVEL

12 14

15 T! 11 11

Flow Research Report No. 178

Arctic Mechanical Energy Budget.

Contract N00914-79-C-0147

15

By
J. J. Kolle

11 December 1980

Flow Research Company
A Division of Flow Industries, Inc.
21414 - 68th Avenue South
Kent, Washington 98031
(206) 872-8500

DTIC
ELECTE
S AUG 24 1981 D
D

DISTRIBUTION STATEMENT A
Approved for public release;
Distribution Unlimited

390401

Table of Contents

	Page
1. Introduction	1
2. Mechanical Energy Balance in the PBL and OML	6
3. Waves in Sea Ice	11
4. Mechanical Energy Balance for Waves	13
5. Mechanical Energy Balance for Sea Ice	18
6. Flow Chart Description	21
7. Magnitudes of Transfer Terms	26
8. Discussion	31
9. Conclusion	34
Appendix	35
References	38

Arctic Mechanical Energy Budget

1. Introduction

The transfer of mechanical energy from the atmosphere into the ocean is responsible for the bulk of waves and currents observed. In the Arctic the rate of transfer will be greatly altered by the presence of an ice cover. It is useful to have an estimate of the energy available to drive currents in the Arctic when constructing large scale circulation models. We shall see that the ice cover greatly reduces the available energy in some cases. Energy which is transferred to the ice is responsible for its motion and deformation. Both are important considerations for shipping, military operations and resource recovery in the Arctic. Noise generation by ice deformation can be directly related to mechanical energy available.

Mechanical energy flows from the atmosphere into the ocean. The source of this energy is solar radiation which drives the global atmospheric heat engine. Work is done on the atmosphere and large scale pressure gradients develop. The pressure gradient potential energy may thus be taken as a starting point in tracing the flow of atmospheric mechanical energy.

In the upper atmosphere, far from the effects of the surface, the balance of pressure gradient and Coriolis force causes a geostrophic wind. At the ocean surface winds must be equal to the current and thus small. The transition region is a layer of variable height known as the planetary boundary layer (PBL). Energy is transferred from this layer through its bottom boundary to the surface of the ocean.

Energy may be transferred to waves on the surface or to ice motions. Waves may also be generated in the ice cover. In the treatment that follows the word "layer" is used to define the mode of mechanical energy being considered. Thus, mechanical energy carried by the ice is referred to as being contained in the ice layer while the wave mechanical energy is contained in the wave layer. In the latter case this is somewhat of a misnomer since the kinetic energy of a wave, though dropping exponentially, extends to the bottom. None-the-less, it is useful to think of the ice

and waves as surface layers which mediate the flow of mechanical energy into the ocean.

A schematic drawing of the energy flow paths is shown in Figure 1. Some of the energy in the PBL is transferred directly to currents in the top layer of the ocean. This layer has a strong similarity to the atmospheric PBL (Coantic, 1975). It is defined by the depth to which the surface effects are important and is marked by a uniform temperature and salinity. This region is referred to as the oceanic mixed layer (OML).

Both wave energy and ice M.E. may be transferred to currents and turbulence within the OML. The energy contained in the OML is eventually transferred to the rest of the ocean. This study seeks to understand the effect of the ice cover on the mechanical energy budget of the Arctic. The effect will be limited to the interface region from the top of the PBL to the bottom of the OML since these are the regions of the atmosphere and ocean influenced by the interface.

Each layer may be characterized by a mechanical energy balance equation. For a stationary system the rate of energy input to each layer must equal the output. The energy balance equations are coupled by terms describing transfer from one layer to another. Other terms describe energy transport and dissipation.

The balance and flow of mechanical energy may be most conveniently displayed in a flow chart. This is also a useful way to represent the magnitudes and importance of energy transfer terms (Holland and Lin, 1975). Measurements of mechanical energy parameters are generally made at one point and averaged for some time. Mechanical energy inputs for ocean models requires spatial averages on the model grid scale and temporal averages over the model time increments. It is useful to know the geographic variation of the energy budget term as well as seasonal and extreme values. All these considerations lead to spatial and temporal averaging scales. These allow a useful comparison of mechanical energy flow in different regions of the Arctic at different times.

The horizontal scale should be small enough to resolve the variety of features shown in Figure 2. It should distinguish between open

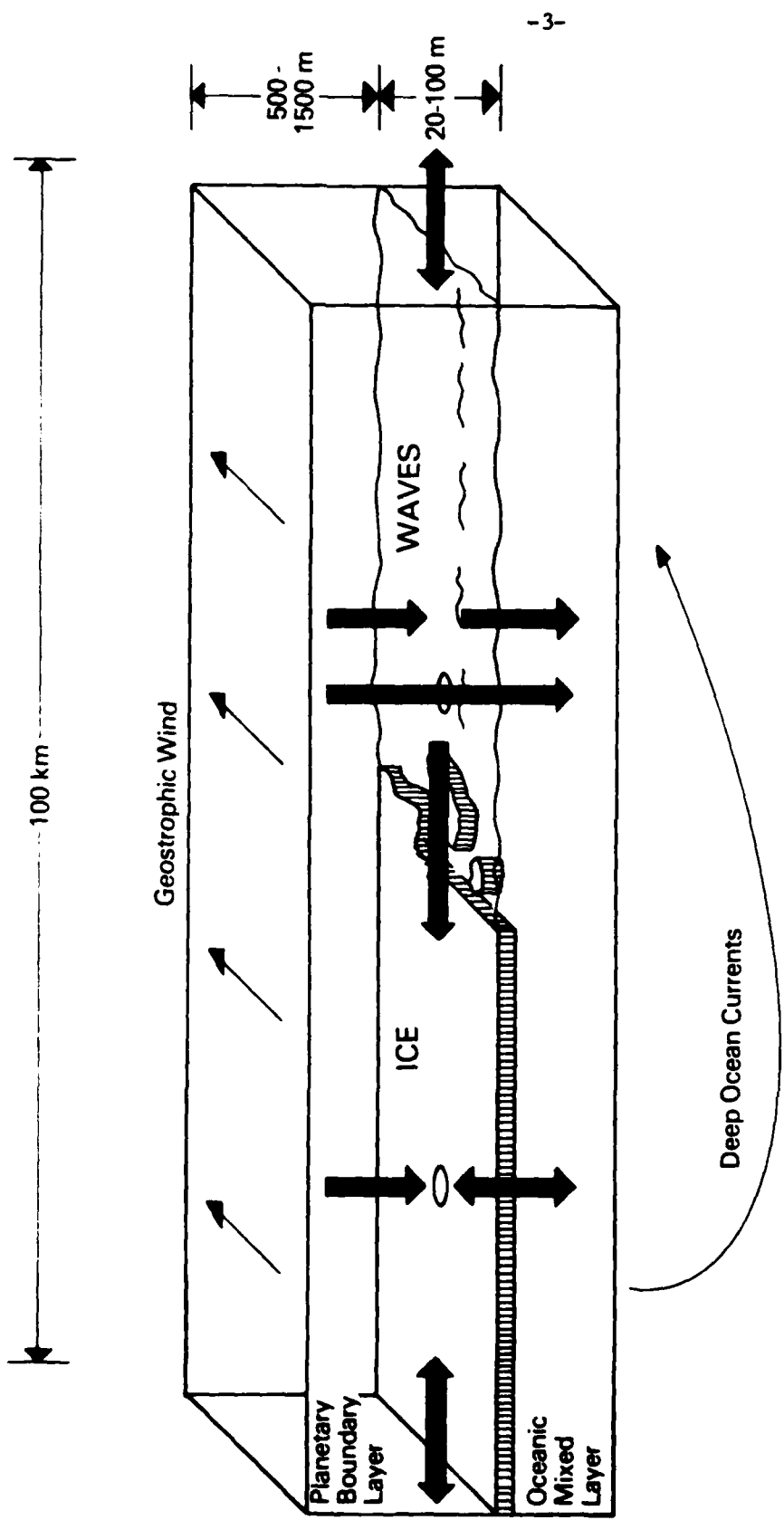


Figure 1. Schematic Drawing of Mechanical Energy Transfer Pathways from the Atmosphere to a Partially Ice Covered Ocean.

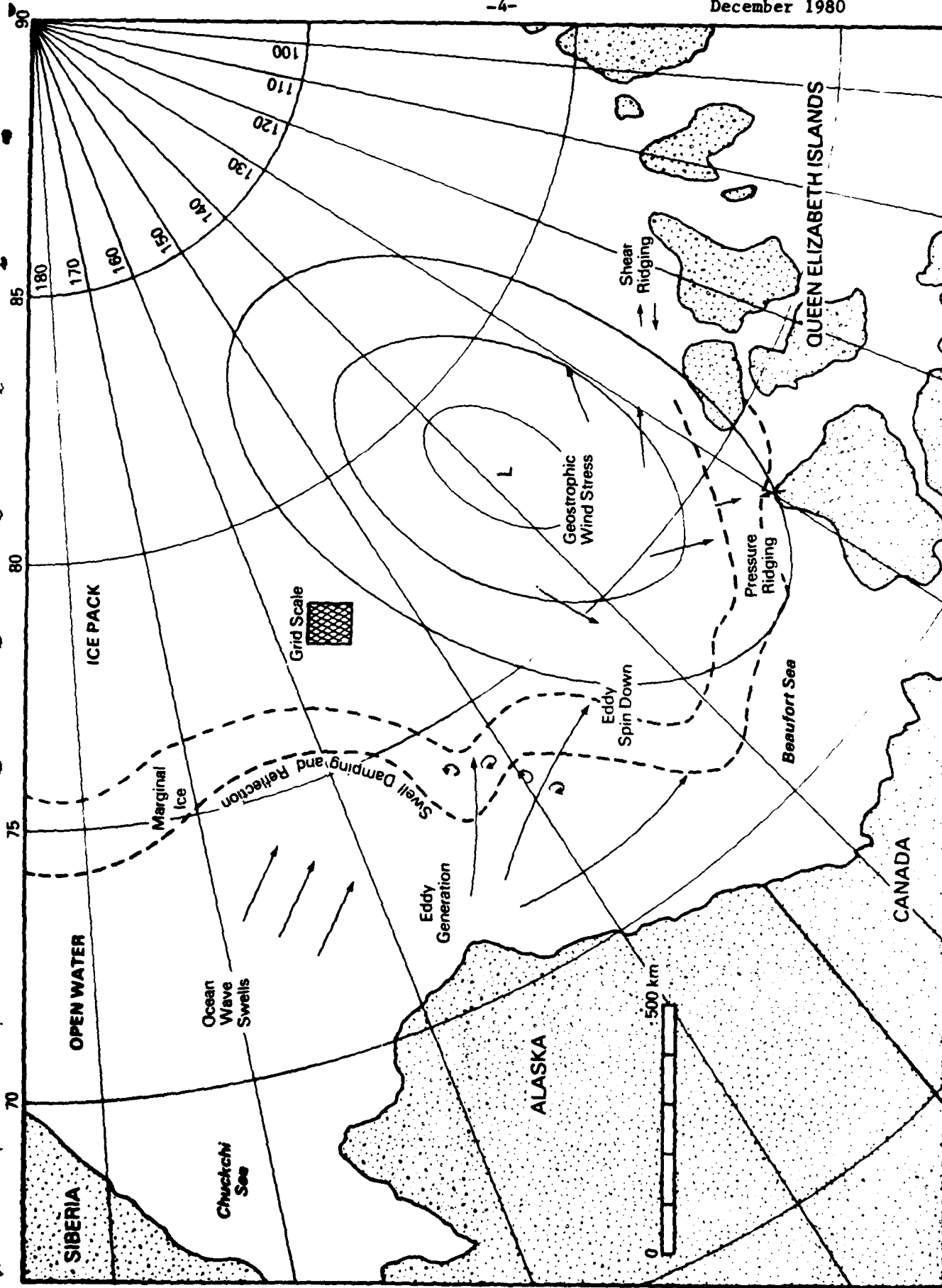


Figure 2. Important Features to be Resolved in an Arctic Mechanical Energy Budget.

water, pack ice and the marginal ice zone (MIZ) as well as regions of intense ice deformation. Furthermore winds and currents should not vary appreciably over the length scale. As long as the scale is less than the scale of synoptic pressure variations this should be the case. Pressure systems in the Arctic have scales of 500 km or greater so that winds will not vary much on a scale of 100 km as is observed. The MIZ zone is about 100 m wide while ridging may be confined to a region a few hundred meters wide. If the scale becomes too small however, one can no longer see the forest for the trees. Ice floes are 10 km or so in diameter. Hibler (1980) holds that averaging ice strains over scales greater than 20 km averages out discontinuities such as leads and shear ridges. An averaging length of ~ 100 km should thus be adequate for the purposes of this work.

Vertical scales are determined by the height of the PBL and the depth of the OML, Figure 1. These are of the order 1000 m and 50 m respectively (Coantic, 1975) though considerable variation is seen in both layers both in time and space. The vertical scale is thus much smaller than the horizontal. Terms in the energy balance may now be calculated by integrating the relevant parameters over the height of the various layers shown in Figure 1. Energy densities are thus expressed in terms of energy per unit area.

There are essentially two seasons in the Arctic, winter when the ocean is almost entirely ice covered and summer when large areas are ice free. Seasonal variations will be described by averages taken over periods of 20 to 60 days. This is long enough to smooth out daily fluctuations due to storms and still short enough to resolve the season. Extreme values due to storms are of interest as well. These may be resolved by taking averages over a day since synoptic events last for periods of a few days.

In this paper the mechanical energy budgets for the PBL, ice pack, waves and OML are presented and integrated over the appropriate spatial and temporal scales. Magnitude estimates of the various terms in these budgets are made based on the parameters compiled in Appendix 1. These estimates vary with geography and season. A final section uses a flow chart format to make comparisons between energy flow in the two Arctic

seasons and for open water, marginal ice zone and central ice pack. These comparisons give an insight into the effect of sea ice on mechanical energy transistor processes and, hopefully, will provide future workers with a qualitative guide.

The main source of energy for oceanic circulation is the atmosphere. Some additional energy is supplied by tides. Tides are an important energy source for currents in shallow waters which are sheltered from the atmosphere by an ice cover. They are responsible for tidal cracks in the fast ice. However, tidal components in the Arctic are small, (Callaway, 1976) vanishing at the pole. For the most part they provide an insignificant background kinetic energy which is uniform in space and time for averaging periods of 12 hours or more. The various mechanisms by which tidal energy may transferred to eddies and internal waves are beyond the scope of this work.

2. Mechanical Energy Balance in the PBL and OML

The mechanical energy balance for the PBL and OML may be derived from the classical Navier-Stokes force balance equation for a fluid. If the fluid velocity is \tilde{u} ,

$$\rho \frac{d}{dt} \tilde{u} + 2\rho \tilde{\Omega} \tilde{x} \tilde{u} + \rho \nabla \tilde{x} + \nabla p = \nabla \cdot \tilde{\sigma} \quad (2.1)$$

where $\tilde{\Omega}$ is the earths angular velocity which gives rise to the Coriolus force, \tilde{x} is the gravitational potential, p is the pressure field and $\tilde{\sigma}$ is the viscous stress tensor

$$\tilde{\sigma} = 2\tilde{u} \tilde{D} \quad (2.2)$$

where

$$\tilde{D} = \frac{1}{2} (\nabla \tilde{u} + \nabla^t \tilde{u}) \quad (2.3)$$

is the stretching. Taking the scalar product of this equation with velocity gives a balance equation for kinetic and potential mechanical energy,

$$\rho \frac{d}{dt} \left(\frac{1}{2} \tilde{u} \cdot \tilde{u} + \tilde{x} \right) = - \tilde{u} \cdot \nabla p + \tilde{u} \cdot (\nabla \cdot \tilde{\sigma}) . \quad (2.4)$$

The change in potential energy all goes into gravitational work,

$$\rho \frac{d\chi}{dt} = \rho \tilde{u} \cdot g \quad (2.5)$$

the other terms express the work done against pressure gradients

$$= - \tilde{u} \cdot \nabla p \quad (2.6)$$

and viscous forces

$$= \tilde{u} \cdot (\nabla \cdot \tilde{\sigma}) . \quad (2.7)$$

In turbulent systems such as the atmosphere or ocean it is necessary to describe high frequency velocity components statistically. The velocity vector may be described by its mean and fluctuating parts

$$\tilde{u} = \bar{u} + \tilde{u}' . \quad (2.8)$$

In compressible gases it is best to define the mean as a mass weighted average,

$$\bar{u} = \frac{\overline{\rho u}}{\overline{\rho}} \quad (2.9)$$

where the bar indicates the conventional averaging operator. The mass weighted averaging leads to a clear separation between the mean and turbulent kinetic energies

$$\frac{1}{2} \overline{\rho \tilde{u} \cdot \tilde{u}} = \frac{1}{2} \overline{\rho \bar{u} \cdot \bar{u}} + \frac{1}{2} \overline{\rho \tilde{u}' \cdot \tilde{u}'} . \quad (2.10)$$

The mean mechanical energy balance equation may be obtained from the scalar product of \bar{u} and the mean momentum balance equation,

$$\overline{\rho} \frac{d\bar{u}}{dt} = - \overline{\rho} \nabla \chi - 2 \overline{\rho} \tilde{\sigma} \cdot \bar{u} - \nabla \bar{p} + \nabla \cdot \overline{\tilde{\sigma}} + \nabla \cdot \overline{\tau} \quad (2.11)$$

which is essentially the same as the total momentum balance equation except for the term containing

$$\tau = - \overline{\rho u' \times u'} \quad (2.12)$$

representing turbulent Reynold stresses. The mean mechanical energy balance equation is then

$$\overline{\frac{d}{dt} \left(\frac{1}{2} \overline{u \cdot u} \right)} = - \overline{\rho u \cdot g} - \overline{u \cdot \nabla p} + \overline{u \cdot (\nabla \cdot \overline{u})} + \overline{u \cdot (\nabla \cdot \tau)} . \quad (2.13)$$

The last term may be rewritten using the chain rule

$$\overline{u \cdot (\nabla \cdot \tau)} = \nabla \cdot (\overline{\tau \cdot u}) - \text{tr} \overline{\tau D} . \quad (2.14)$$

The first of these is the divergence of a stress flux and represents the rate at which turbulence kinetic energy is transferred into or out of a unit volume by the mean flow. The second is the rate at which turbulence energy is being produced by shear in the mean flow and is known as the mechanical production term.

It is reasonable to assume zero vertical component for the long term mean flow in both boundary layers. Then

$$- \overline{\rho u \cdot g} = 0 \quad (2.15)$$

which is to say the mean flow on average does no gravity work. The rest of the terms may be evaluated by integrating over the volume of each layer, V_L

$$\int_{V_L} \overline{\frac{d}{dt} \left(\frac{1}{2} \overline{u \cdot u} \right)} dV = - \int_{V_L} \overline{u \cdot \nabla p} dV + \int_{V_L} \overline{u \cdot (\nabla \cdot \overline{u})} dV + \int_{V_L} \nabla \cdot (\overline{\tau \cdot u}) - \text{tr} \overline{\tau D} dV \quad (2.16)$$

viscous forces are important only in small scale motions (Phillips, 1966) and may be neglected in the mean balance for both the atmosphere and ocean boundary layers,

$$\int_{V_L} \mathbf{U} \cdot (\nabla \cdot \mathbf{g}) dv \sim 0 . \quad (2.17)$$

For the horizontal scale chosen, the mean velocity may be considered to vary only with height. For the purposes of this estimate it is assumed that the turbulence stress tensor is horizontally homogeneous. The mechanical energy balance equation may then be written in terms of the energy flow per unit horizontal area. For a PBL of height h ,

$$\int_0^h \bar{\tau} \frac{d}{dt} \left(\frac{1}{2} \mathbf{U} \cdot \mathbf{U} \right) dz = - \int_0^h \mathbf{U} \cdot \nabla \bar{p} dz + \int_0^h \left(\frac{\partial}{\partial z} (\mathbf{k} \cdot \bar{\tau} \cdot \mathbf{U}) - \text{tr} \bar{\tau} D \right) dz \quad (2.18)$$

where \mathbf{k} is a unit vector normal to the surface. The Reynolds stress flux gradient gives the power input at the top and bottom of the layer

$$\int_0^h \frac{\partial}{\partial z} (\mathbf{k} \cdot \bar{\tau} \cdot \mathbf{U}) dz = \bar{\tau}_h \cdot \mathbf{U}_h - \bar{\tau}_0 \cdot \mathbf{U}_0 . \quad (2.19)$$

It is commonly assumed that the Reynolds stress at the top of the PBL is zero (Roll, 1965). For the purposes of estimation it may also be assumed that the density and pressure gradients are constant over the height of the PBL (Hunkins, 1980). The balance of mean kinetic energy for the PBL may then be written

$$\frac{d}{dt} \int_0^h \left(\frac{1}{2} \rho \mathbf{U} \cdot \mathbf{U} \right) dz = - \int_0^h \mathbf{U} \cdot \nabla \bar{p} dz - \bar{\tau}_0 \cdot \mathbf{U}_0 - \int_0^h \text{tr} \bar{\tau} D dz . \quad (2.20)$$

For a stationary system

$$\frac{d}{dt} KE = \frac{d}{dt} \int_0^h \left(\frac{1}{2} \rho \mathbf{U} \cdot \mathbf{U} \right) dz = 0 \quad (2.21)$$

and

$$\int_0^h \mathbf{U} \cdot \nabla \bar{p} dz = - \bar{\tau}_0 \cdot \mathbf{U}_0 - \int_0^h \text{tr} \bar{\tau} D dz . \quad (2.22)$$

-10-

The term on the left is the rate of working by the mean flow on the pressure gradient. This is partially balanced by the Reynolds stress at the bottom surface

$$-\bar{\tau}_0 \cdot \bar{U}_0 = + \overline{\rho \bar{u}' \times \bar{u}' \cdot \bar{U}_0} \quad (2.23)$$

where \bar{U}_0 is the velocity of the water or ice at the bottom of the boundary layer.

The last term is the vertical average areal density of rate of turbulence kinetic energy production. This is the mechanical production term averaged over the height of the PBL. This turbulent kinetic energy eventually travels through a turbulence energy cascade whereby the wavelengths of disturbances become progressively smaller (Lumley and Panofsky, 1965). Eventually the scale of motion becomes small enough that the energy is dissipated by viscous heating. Some of the turbulent kinetic energy may be transferred to waves and turbulence in the oceanic mixed layer through work done by turbulent pressure variations on the sea surface. Large scale pressure variations also provide an energy source for the ocean but these are not associated with boundary layer transfer.

Mechanical Energy Balance in the OML

The mean mechanical energy balance for the mixed layer may be handled in the same way as for the PBL. Vertical integration now extends from the bottom of the layer to the surface or bottom of the ice. The mean flow is considered to be essentially horizontal (Phillips, 1966)

$$\frac{d}{dt} \int_{-d}^0 \left(\frac{1}{2} \bar{\rho} \bar{U} \cdot \bar{U} \right) dz = - \int_{-d}^0 \bar{U} \cdot \nabla p dz + \int_{-d}^0 \left(\frac{\partial}{\partial z} \left(\bar{k} \cdot \bar{\tau} \cdot \bar{U} \right) - \text{tr} \bar{\tau} D \right) dz \quad (2.24)$$

One of the characteristics of the mixed layer is a uniform density. The pressure gradient is related to the sea surface tilt ∇H

$$\nabla p = \rho g \nabla H \quad (2.25)$$

and is uniform with depth. Assuming no turbulence at the bottom of the mixed layer gives zero Reynolds stress here. The energy balance becomes

$$\frac{d}{dt} \int_{-d}^0 \frac{1}{2} \bar{U} \cdot \bar{U} dz = - \int_{-d}^0 \bar{U} \cdot \rho g \nabla H dz + \bar{z}_0 \cdot \bar{U}_0 - \int_{-d}^0 \tau r \bar{\tau} D dz . \quad (2.26)$$

The stationary balance is

$$\bar{z}_0 \cdot \bar{U}_0 = \int_{-d}^0 \bar{U} \cdot \rho g \nabla H dz + \int_{-d}^0 \tau r \bar{\tau} D dz \quad (2.27)$$

The surface stress power input is balanced by changes in sea surface tilt and by turbulent dissipation of energy. In open water the surface stress is just the Reynolds stress due to shear in the atmosphere. These stresses must be equal and opposite in direction for equilibrium to occur. Underneath the ice, the stress is due to drag by relative motion of the ice sheet.

Sea surface tilt may be either a source or sink of energy. The tilt due to geostrophic pressure variations does work on the mean flow. On the other hand some of the energy of currents is transferred temporarily into changes in sea surface potential.

Turbulence is generated in the OML, as in the PBL, by shear in the mean flow. Other sources of turbulence in the mixed layer are direct pumping of turbulent motions by atmospheric turbulence and turbulence generated by breaking waves. The first of these is thought to be small. Breaking of waves may represent a large part of the turbulence energy flux to the ocean. The turbulence, however, is limited to the near surface within a distance comparable to the wavelength of the breaking wave (Phillips, 1966). This dissipation process is considered in the wave energy balance.

3. Waves in Sea Ice

Waves in open water near an ice pack will transfer some of their energy to the ice by propagating into it. Long period waves may propagate hundreds of kilometers into the pack (Robin, 1963). Wadhams (1973) gives an expression for the ratio of transmitted to reflected wave energy density for waves impinging on an ice sheet.

$$R = 1 + \frac{32 Eh^{3/4}}{3\pi g^{1/4} (1-\nu^2)} \quad (3.1)$$

where h is the half thickness of the ice

E is Youngs modulus

and λ is the wavelength.

Long periods are most effective at penetrating the ice with essentially all the energy of a 16 s wave being transmitted into 2.5 m thick ice. The ratio goes as λ^4 so that only 25 percent of the energy of 5 s waves penetrates.

The periods of waves which can be generated by a storm are limited by the fetch over which the wind blows. Waves with periods longer than 5 require fetches of a hundred kilometers or more to gain significant energy. Open leads and polynyas in the Arctic have fetches which are limited to a few kilometers except for the large semipermanent polynyas. For the most part, storms over open leads or polynyas should not generate long swells. The wave energy generated within a lead will thus be reflected and scattered by the ice margin.

It is possible that storms over large open fetches of water such as the Chukchi or Norwegian seas could generate significant long period swells which would in turn transfer large amounts of energy to the marginal sea ice zone.

When a wave swell travels under the ice, part of its energy is taken up as a flexural gravity wave in the ice sheet. Attenuation of this wave occurs due to creep in the ice and perhaps by fracture as well. Wadhams (1973) derives the rate at which the wave energy decays with penetration into the sheet. Assuming a flow law for ice of the form

$$\frac{d\tilde{\epsilon}}{dt} = \frac{\tau^{n-1}}{B^n} \tilde{\sigma}' \quad (3.2)$$

where $\tilde{\epsilon}$ is the strain tensor

$\tilde{\sigma}'$ is the deviatoric stress tensor

$\tau = \frac{1}{2} |\tilde{\sigma}' \cdot \tilde{\sigma}'|^{1/2}$ is the effective shear stress

B = some function of temperature

n = a constant usually taken to be 3

And given a wave profile

$$\xi = A \sin 2\pi (x/\lambda - t/T) \quad (3.3)$$

for a wavelength, λ , and period, T . The rate at which energy is lost in an ice sheet of thickness h per unit area is

$$\frac{dQ}{dt} = 2 \frac{4\pi^2 E |\xi| / \lambda^2 (1 - v^2)^{n+1} h^{n+2}}{(2\bar{B})^n (n + 2)} \quad (3.4)$$

with E = Young's modulus for sea ice ~ 6 GPa

v = Poissons ratio = 0.3 (Lavrov, 1969)

and $\bar{B} = \frac{1}{h} \int_0^h B dz$ is the vertical average of B . Wadhams estimates

B from studies of wave attenuation to be between 10^7 and $10^8 \frac{\text{kg.s}}{\text{m}}$.

The energy loss may be averaged over an entire wave

$$\frac{dQ}{dt} = 2 \frac{2\pi^2 EA / \lambda^2 (1 - v^2)^{n+1} h^{n+2}}{(2\bar{B})^n (n + 2)} \quad (3.5)$$

An incident wave height of 10 m represents an upper bound on the largest swells which are liable to enter the ice. For a 16s wave, $\lambda = 400$ m. The energy dissipation rate at the ice margin is 500 watt/m^2 . For comparison a 1 m wave dissipates only 0.5 watt/m^2 . Dissipation rates fall off rapidly with distance from the ice edge. Observations of waves with periods from 10-60 seconds more than 100 km from the ice margin give maximum wave heights of 1 cm for a dissipation rate of $5 \times 10^{-10} \text{ watt/m}^2$.

4. Mechanical Energy Balance for Waves

At the free surface of an incompressible, irrotational fluid the dynamic boundary condition is,

$$\frac{\partial P}{\partial t} = \frac{\partial \phi}{\partial t} \Big|_{z=\eta} + \frac{1}{2} \tilde{u} \cdot \tilde{u} \Big|_{z=\eta} g\eta \quad (4.1)$$

where ϕ is a velocity potential,

$$\mathbf{u} = \nabla \phi \quad (4.2)$$

satisfying Laplaces equation,

$$\nabla^2 \phi = 0 \quad (4.3)$$

and η is the elevation of the free surface above some reference height.
Let a dot stand for differentiation with respect to time,

$$\dot{\eta} = \frac{\partial \eta}{\partial t} \quad . \quad (4.4)$$

Multiplying Bernoulli's equation with the surface velocity, $\dot{\eta}$ and averaging over a unit area gives a balance equation for transfer of energy across the interface,

$$-\overline{p\dot{\eta}} = \overline{\rho\phi\dot{\eta}} \Big|_{z=\eta} + \frac{\rho}{2} \overline{\mathbf{u} \cdot \mathbf{u}} \Big|_{z=\eta} + \overline{pg\eta\dot{\eta}} \quad (4.5)$$

The term

$$-\overline{p\dot{\eta}} = R_E \quad (4.6)$$

is the rate at which the atmosphere does work on the waves through the product of pressure on the free surface and the free surface velocity.

The rate of change of mean kinetic energy per unit horizontal area of a wave is given by Kinsman (1965, p. 524)

$$\dot{T} = \overline{\rho\dot{\phi}\dot{\eta}} + \frac{1}{2} \overline{\rho u^2 \dot{\eta}} - \nabla_H \cdot \mathbf{F} \quad (4.7)$$

where

$$\overline{F} = - \int_{-\infty}^{\eta} \rho \dot{\phi} u dZ , \quad (4.8)$$

is the horizontal energy flux vector representing the mean energy flux per unit horizontal surface length. The energy balance at the surface $z = \eta$ may thus be rewritten

$$\dot{T} = \overline{p \dot{n}} + \nabla_H \cdot \overline{F} - \overline{g n \dot{n}} . \quad (4.9)$$

The energy transferred across the surface by \dot{n} is then up by Kinetic energy, \dot{T} , potential energy

$$\dot{V} = \overline{g n \dot{n}} , \quad (4.10)$$

and horizontal energy flux, $\nabla_H \cdot \overline{F}$.

In reality the mechanical energy budget must be more complex than is indicated by Equation 4.9. The driving force is the Reynolds stress due to wind shear. This stress includes both work done by small scale pressure and shear stresses on the surface Phillips (1977) suggests however that normal stresses provide the dominant means of energy transfer to waves. Work is done by the component of pressure in phase with the wave. The difficulty comes in calculating the average energy flux. The rate of energy flux to the waves is strongly dependent upon the wave structure which depends in turn on the turbulence. The momentum flux to waves may be estimated from

$$\tau_w = 2.5 \times 10^{-2} \rho_a u^2 s^2 \quad (\text{Phillips, 1977}) \quad (4.11)$$

where u is the wind at some reference height, usually 10 meters, and s^2 is the mean square slope of the waves, at saturation

$$s^2 \approx 1.4 \times 10^{-2} . \quad (4.12)$$

This gives

$$\tau_w \approx 3.5 \times 10^{-4} \rho_a u^2 \quad (4.13)$$

equivalent to a wave drag coefficient

$$C_w = 3.5 \times 10^{-4} \quad . \quad (4.14)$$

This may be compared to the drag coefficient giving the surface shear stress

$$\tau_o = C_z \rho_a u_z^2 \quad (4.15)$$

with

$$C_{10} = 1.5 \times 10^{-3} \quad . \quad (4.16)$$

The momentum flux to waves is thus about one fifth the flux to currents. Mechanical energy transfer may be much larger however since power density is the product of stress and velocity. In the case of waves the appropriate velocity is the phase velocity which is much larger than the water surface velocity.

The wave energy, $E = T + V$, is dissipated by viscosity and wave breaking. Phillips (1977) gives an attenuation coefficient

$$\gamma_v = \frac{\partial E}{\partial t} \quad 2E = 2v/\kappa \quad (4.17)$$

relating the energy loss rate to the energy contained by a given wave number, κ , and the viscosity.

In order to evaluate the total energy dissipation rate integrated over all wave numbers the wave spectrum must be known as well as the amplitude of the waves. For the most part however, the viscous attenuation term is small especially at low wavenumbers where the mechanical energy of ocean waves is concentrated. Phillips (1977, p. 54) gives attenuation

coefficients as a function of wave number. On a clean surface a wave with wavelength $\lambda = 1 \text{ m}$ or more has an attenuation coefficient of less than $2 \times 10^{-4} \text{ s}^{-1}$. For this reason attenuation is not considered important in most descriptions of gravity waves. On the other hand it is possible for low frequency waves to feed energy into higher frequencies where dissipation occurs.

Other energy may be dissipated by wave breaking. It is difficult to assess the magnitude of this dissipation mechanism. It is most important in the development of a saturated sea state. In this case wave breaking is wide-spread and is responsible for the form of the wave spectrum. Small wavelengths break at amplitudes smaller than large wave lengths giving a saturation spectrum which decays at short wave-lengths (Phillips, 1966, p. 113).

Waves also transfer energy to current through the work of the radiation stress tensor. Its magnitude is related to the energy density of the wave by

$$S_{11} = \frac{1}{2} E(k) \quad (\text{Kraus, 1972}) \quad (4.18)$$

The rate at which the radiation stress does work on a current is the product of radiation stress and current velocity gradient. The energy density of the waves also increases as they pass into an opposing current by geometric convergence. A wave of velocity C_0 and energy density E_0 which moves into a current, u , has a new phase speed

$$C = C_0 \left[\frac{1}{2} + \frac{1}{2} \left(1 + \frac{4u}{C_0} \right)^{\frac{1}{2}} \right] \quad (4.19)$$

and energy

$$E = \frac{E_0 C_0^2}{C(C + 2u)} \quad (4.20)$$

The rate at which the waves work on a current is

$$\frac{-\partial E}{\partial t} = \frac{\partial E}{\partial x} (u + \frac{1}{2} C) + \frac{1}{2} E \frac{\partial u}{\partial x} \quad (\text{Phillips, 1966}) \quad (4.21)$$

This last term may be added to the steady state mechanical energy balance equation, $\dot{T} = 0$, $\dot{V} = 0$,

$$-\tau_w \dot{n} = \nabla_H \cdot F + - (u + \frac{1}{2} C) \frac{\partial E}{\partial x} - \frac{1}{2} E \frac{\partial n}{\partial x} - \varepsilon \quad (4.22)$$

note that P has been replaced by τ_w as a more complete surface stress representation. Dissipation by wave breaking is included as an unknown function, ε .

5. Mechanical Energy Balance for Sea Ice

The momentum balance equation for an area of sea ice may be used to derive the mechanical energy balance. In the plane of the sea ice the two dimensional momentum balance is (Coon and Pritchard, 1979)

$$\dot{m\mathbf{u}} = -2 m \mathbf{\Omega} \wedge \mathbf{u} + \nabla \cdot \mathbf{\sigma} + \mathbf{\tau}_u + \mathbf{\tau}_w - mg \nabla H \quad (5.1)$$

where m is the mass per unit area of sea ice, \mathbf{u} is the horizontal velocity vector, $\mathbf{\Omega}$ is the angular velocity vector at the earth, $\mathbf{\sigma}$ is the Cauchy stress resultant in excess of hydrostatic equilibrium $\mathbf{\tau}_u$ is the traction exerted on the upper surface of the ice by the atmosphere, $\mathbf{\tau}_w$ is the traction on the lower surface due to water drag, g is gravitational acceleration and H is the dynamic sea surface height.

Taking the inner product of the momentum balance with ice velocity gives the mechanical energy balance equation

$$\frac{\partial}{\partial t} \left(\frac{1}{2} m \mathbf{u} \cdot \mathbf{u} \right) = \mathbf{u} \cdot (\nabla \cdot \mathbf{\sigma}) + \mathbf{u} \cdot \mathbf{\tau}_u + \mathbf{u} \cdot \mathbf{\tau}_w - mg \mathbf{u} \cdot \nabla H \quad (5.2)$$

The Coriolus term drops out since the force is perpendicular to the ice motion and thus does no work. The ice is driven by the atmospheric power term,

$$P_a = \mathbf{u} \cdot \mathbf{\tau}_a \quad . \quad (5.3)$$

The ice transfers energy to the ocean at a rate

$$p_w = - \underline{u} \cdot \underline{\tau}_w \quad (5.4)$$

both by exerting drag on the mixed layer. The potential energy of the ice is increased by work done against the dynamic topography

$$p_H = mg \underline{u} \cdot \nabla H \quad (5.5)$$

The remaining term represents the energy input to the ice itself due to divergence of the stress

$$p_I = - \underline{u} \cdot (\nabla \cdot \underline{\sigma}) \quad (5.6)$$

This term may be written

$$\underline{u} \cdot \nabla \cdot \underline{\sigma} = \nabla \cdot (\underline{u} \underline{\sigma}) + \text{tr} \underline{\sigma} \underline{D} \quad (5.7)$$

The first term is the divergence of stress flux; its physical meaning will become more apparent when integrated over the area of the grid. The second term is the trace of the product of stress and stretching. It represents the work done on the ice due to both elastic and plastic deformations. The stretching \underline{D} may be determined from velocity gradients within the grid,

$$\underline{D} = \frac{(\nabla \underline{u} + \nabla^T \underline{u})}{2} \quad (5.8)$$

where T signifies the transpose operation. The rate of work on the ice is thus,

$$p_i = \text{tr} \underline{\sigma} \underline{D} \quad (5.9)$$

and the mechanical energy balance may be written

$$\frac{\partial}{\partial t} \left(\frac{1}{2} m \bar{u} \cdot \bar{u} \right) = \nabla \cdot (\bar{u} \sigma) + p_i + p_u + p_w + p_h \quad (5.10)$$

The mechanical energy balance for the ice layer may be integrated over the area of the ice within a grid element. If we denote this a real average by

$$\bar{\phi} = \frac{1}{A_i} \int \phi \, dA_i \quad (5.11)$$

the integrated equation may be written

$$\frac{\partial}{\partial t} \left(\frac{1}{2} m \bar{u} \cdot \bar{u} \right) = \frac{1}{A_i} \int \nabla \cdot (\bar{u} \sigma) \, dA_i + \bar{p}_i + \bar{p}_w + \bar{p}_a + \bar{p}_h \quad (5.12)$$

The integral of stress flux divergence may be evaluated using the Green-Gauss theorem

$$\frac{1}{A_i} \int \nabla \cdot (\bar{u} \sigma) \, dA_i = \frac{1}{A_i} \int_{\Gamma} (\bar{u} \sigma) \cdot \bar{n} \, d\ell \quad (5.13)$$

This term is thus the rate at which work is transferred to the area A_i by tractions, $\bar{c} \cdot \bar{n}$, on its boundary, Γ ; \bar{n} is a unit normal to the curve Γ .

For the length scale of 100 km chosen the mean 10 m wind may be considered to be a constant over the entire averaging area. This gives a constant wind stress of

$$\bar{\tau}_w = C_{10} |\bar{u}_{10}| \bar{u}_{10} \quad (5.14)$$

where C_{10} is the drag coefficient referenced to the mean 10 m wind velocity \bar{u}_{10} . The mean currents under the ice may also be considered to be constant over the area of a single grid,

$$\bar{\tau}_w = C_w |\bar{u}_w| \bar{u}_w \quad (5.15)$$

The large scale pressure variations which give rise to the dynamic topography are large enough that ∇H may be considered to be constant over the area of the grid (Newton, 1975).

6. Flow Chart Description

The energy transfer mechanisms associated with the power input from the atmosphere to the ocean have been described by four mechanical energy balance equations, Table 1. Each of these equations is coupled to the others; a power output from one equation being an input to another. Keeping track of four energy balance equations simultaneously is unwieldy. Mechanical energy transfer pathways are best described by a flow chart, Figure 3.

This chart represents a steady state flow of energy from the atmosphere into the ocean. The energy density within any given layer is assumed to not change very much over a period of one day. Thus the energy density may be estimated by using daily averages for the relevant parameters. Since average energy density is essentially constant, for a day, its time derivative is zero. The remaining terms in the energy budget must then balance each other. In other words the power input into each layer must equal the power out. The flow chart shows the various transfer (power) terms considered here as inputs and outputs to each layer.

Power input to a layer can arise from one of two sources. An adjacent layer may transfer part of its energy to it. Thus the atmosphere does work on ice, waves and currents and transfers a small fraction of its energy to them. The transfer is uniformly downwards because of the density and velocity contrasts between air and water. Similarly currents may exchange energy with the ice and waves. The energy flow here may change direction, however, and this is indicated by a double arrow on the flow chart. In general the net flux of energy will be into the ocean.

A layer may also be subject to an energy flux due to transmission (as opposed to transfer) of energy within the layer from outside the

Table 1. Mechanical Energy Budgets (Steady State).

Planetary Boundary Layer:

$$0 = - \int_0^h \tilde{u} \cdot \nabla \tilde{r} - \tau_o \cdot \tilde{u}_o - \int_0^h \text{tr} \tau \tilde{D}_a dz$$

Oceanic Mixed Layer:

$$0 = - \tau_o \cdot \tilde{u}_o + \int_{-d}^0 \tilde{u} \cdot pg \nabla H dz + \int_{-d}^0 \text{tr} \tau \tilde{D}_w dz$$

Waves:

$$0 = - \tau_o \cdot \nabla_H \cdot \tilde{F} + (U + \frac{1}{2} C) \frac{\partial E}{\partial x} + \frac{1}{2} E \frac{\partial u}{\partial x} - \varepsilon$$

Ice:

$$0 = \frac{1}{A_i} \int_{\Gamma} (\tilde{u} \cdot \tilde{n}) \cdot \tilde{d}l + \tilde{u} \cdot \tilde{\tau}_a + \tilde{u} \cdot \tilde{\tau}_w + \text{tr} \tilde{\sigma} \tilde{D} + mg \tilde{u} \cdot \nabla H$$

in each equation the velocities are given by \tilde{u} and tractions at the interfaces by $\tilde{\tau}$.

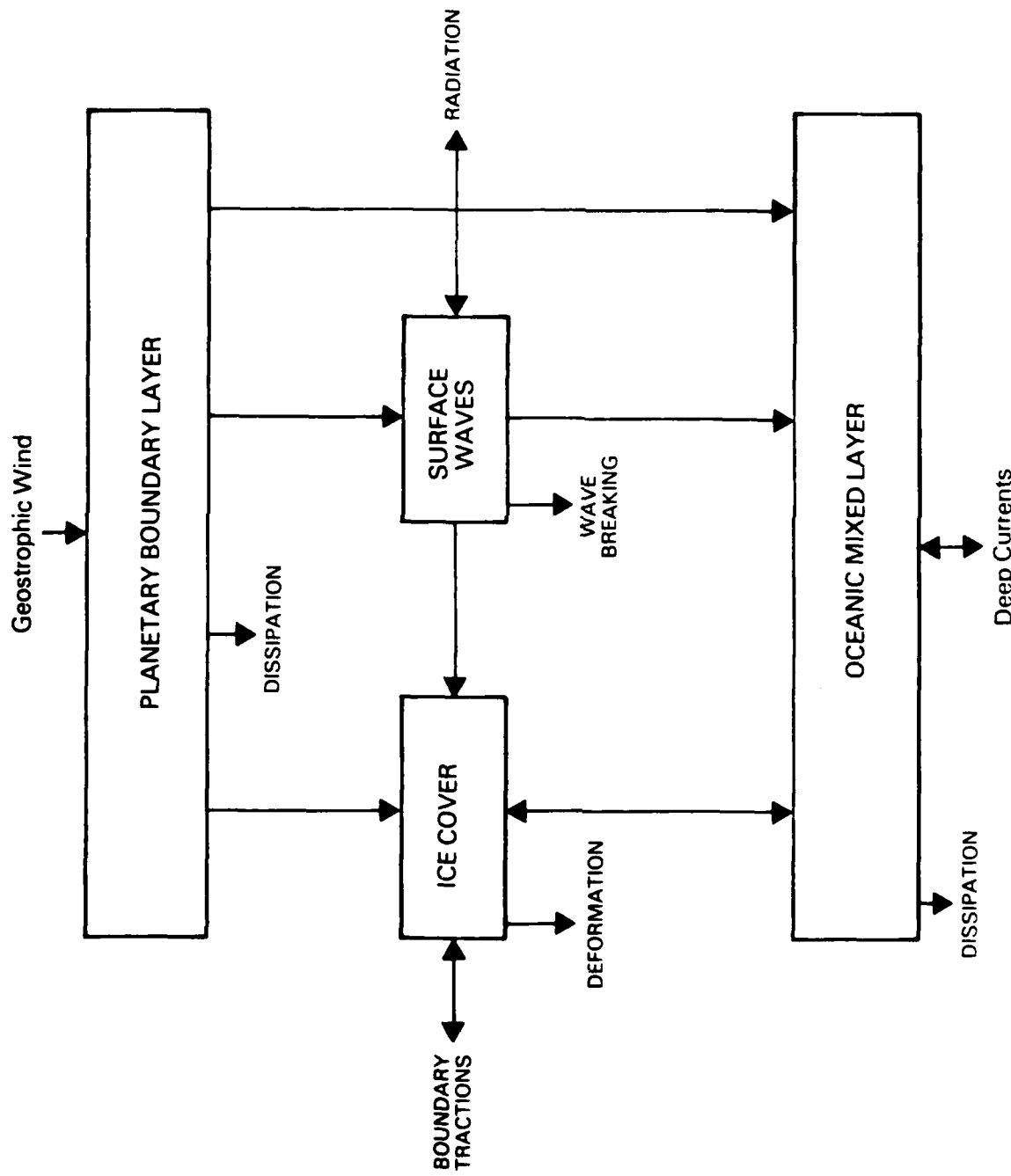


Figure 3. Chart of Mechanical Energy flow from the Atmosphere into a Partially Ice-Covered Ocean.

grid. This is particularly important in the ice where boundary tractions can cause significant energy to be transferred over hundreds of kilometers. Long period waves will also transmit energy over longer distances under some conditions. This energy input mechanism is referred to as lateral flux in the flow chart. This flux may be either positive or negative as indicated by the double arrows in Figure 3. No lateral flux terms are included for the two boundary layers. In both the PBL and OML velocity gradients are much larger in the vertical direction than horizontally. Furthermore the horizontal surfaces through which energy is transferred are much larger than the lateral layer boundaries. Both of these considerations imply that lateral energy flux within these layers is negligible compared to the vertical fluxes.

The flow chart includes a term for transfer of energy between waves and ice. The magnitude of this transfer has been shown to be small with most of the wave energy reflected from the ice. However, the fracturing of ice by ocean swells is important for noise generation in the marginal ice zone and for inducing breakup of the ice pack in spring. The term is thus included for comparison at different localities and seasons.

Each layer may lose energy by transfer or transmission. In fact most of the energy lost will be seen to be due to various dissipation mechanisms. In the boundary layers and waves dissipation occurs when the turbulence energy cascade transfers mechanical energy to turbulent motions of constantly decreasing wavelength. Eventually the wavelengths approach molecular scales and the viscosity of the medium dissipates the energy as heat.

Deformation of the ice pack also dissipates energy; as heat due to the friction of the ice as it grinds against itself and as potential energy stored in ridge-keel systems. This potential energy is lost when the ice melts and in fact adds a minuscule amount of heat during the melting process. All of the terms considered in the mechanical energy budget are orders of magnitude smaller than the fluxes of heat

due to radiation and phase changes considered in a thermal energy budget.

The dissipation terms are the most difficult to measure. An absolute measure would require the detection of small changes of heat flux in a system overwhelmed by much larger changes. Some measures of turbulence dissipation have been made in the atmosphere. For the most part the dissipation term is considered as a residual in energy balance equations where all the other terms are measured.

Measurements of energy dissipation by turbulence in the upper layer of the ocean and by wave generated turbulence are essentially non-existent due to the limitations of transducers. Again these quantities are given as residuals. It is possible to measure the potential energy of ridges and keels directly and these estimates are included here.

The plastic properties of ice as measured in the laboratory may be used in combination with ice dynamics results to estimate the dissipation rates due to ice strains.

7. Magnitudes of Transfer Terms

The source of energy for winds in the PBL is the pressure gradient. This term gives rise to a geostrophic wind which is independent of the surface conditions, be it ice covered or open water. Furthermore, the geostrophic wind is essentially independent of season in the Arctic (Albright, 1980). The energy input to the mean flow in the boundary layer is given by the scalar product of pressure gradient and mean wind integrated over the thickness of the layer,

$$P_G, PBL = \int_0^h u \cdot P dz \quad (7.1)$$

At the top of the PBL the wind is geostrophic and perpendicular to the pressure gradient so that no work is done. The wind turns as it approaches the bottom of the layer by an angle, γ , at about 20° (Carsey, 1980) in the Arctic. The turning angle is a function of the stability at the atmosphere varying from 10° to 50° with increasing stability (Brown, 1980). In general the atmosphere over sea ice is stable since the ice acts to insulate the atmosphere from heating by the ocean. Strong instability may occur in winter over open leads and polynyas where the ocean provides large amounts of heat to the atmosphere.

The Eckman-Taylor model may be used to provide a crude approximation to the energy delivered to the PBL. If the geostrophic wind is G the velocity parallel to the pressure gradient is

$$u_p(z) = G (1 - e^{-\kappa z} \cos \kappa z) \quad (7.2)$$

where $\kappa = (f/2v)^{1/2}$ is the Eckman depth which depends on the Coriolis parameter f and the eddy viscosity v . This expression may be integrated through the Eckman depth for a reasonable approximation to the average velocity parallel to pressure gradient in the boundary layer,

$$\bar{u}_p(z) = \kappa \int_0^{1/\kappa} u(z) dz \quad (7.3a)$$

-27-

$$= \kappa \int_0^{1/\kappa} G (1 - e^{-\kappa z} \cos \kappa z) dz \quad (7.3b)$$

$$= G \left[-\frac{e^{-1}}{z} (\sin 1 - \cos 1) \right] \quad (7.3c)$$

$$\bar{u}_p = .45 G \quad (7.3d)$$

The annual mean geostrophic wind during AIDEX (1975-1976) was

$$G = 8.8 \text{ m/s} \quad (7.4)$$

which gives

$$\bar{u}_p(z) = 4.0 \text{ m/s} \quad (7.5)$$

The geostrophic wind magnitude is related to horizontal pressure gradient by

$$|G| = \frac{1}{\rho_a f} |\nabla_h p| \quad (7.6)$$

$$f = 2\Omega \sin \phi \sim -1.4 \times 10^{-4} \text{ s}^{-1} \text{ at } 76^\circ \text{ N latitude}$$

$$\rho_a = 1.3 \frac{\text{kg}}{\text{m}^3}$$

Then

$$|\nabla_h p| \approx 1.6 \times 10^{-3} \text{ Pa/m} \quad (7.7)$$

Finally the work done on the PBL per unit area may be estimated from

$$P_{G,PBL} = \int_0^h \bar{u}_p(z) dz \cdot \nabla p \sim \kappa \bar{u}_p |\nabla_h p| \quad (7.8a)$$

$$\sim 6.3 \kappa \frac{\text{mwatt}}{\text{m}} \quad (7.8b)$$

typically the height of the PBL is 10^3 m so the total power input is

$$P_G, PBL \approx 6 \frac{\text{watt}}{\text{m}^2} \quad (7.9)$$

Stability conditions can effect this value in two ways. At low stabilities the turning angle is low and the pressure gradient cannot do much work. On the other hand, the height of the PBL increases under these conditions so that the total work done over the layer thickness may be larger.

Reynolds Stress Work

The work done by the PBL on the surface of the ocean is simply the product of Reynolds stress and the appropriate surface velocity. Ice and current velocities are typically about 2% of the 10 meter wind and are turned at about 40° to the right of it in summer (McPhee 1980). The velocity component parallel to the geostrophic wind is thus

$$u_p \approx u_{10} (.02) \cos 40^\circ \quad (7.10)$$

or

$$u_p \approx .015 u_{10} \quad (7.10a)$$

The power is obtained by multiplying by the Reynolds stress.

$$\tau_a = \rho_a C_{10} u_{10}^2 \quad (7.11)$$

$$\tau_a u_p = .015 \rho_a C_{10} u_{10}^3 \quad (7.12)$$

Typically u_{10} is 0.5 m/s which gives a transfer power of $\tau_a u_p \approx 5 \text{ m watt/m}^2$. This is just a small fraction (~.1%) of the energy input into the PBL. The remainder of the energy must be dissipated by the turbulent energy cascade within the PBL. Extreme winds of 20 m/s are occasionally observed in the Arctic. The power input to the ice

-29-

input to the ice by such a wind would be,

$$\tau_a u_p \sim 300 \frac{\text{mwatt}}{\text{m}^2} \quad (7.13)$$

The energy available in the PBL will also be higher, assuming that the geostrophic wind is ~40 m/s gives

$$P_{G, \text{PBL}} \sim 25 \frac{\text{watt}}{\text{m}^2} \quad (\sim 1\% \text{ available power}) \quad (7.14)$$

In the winter the ice velocity is about $0.0065 u_{10}$ (McPhee, 1980). The typical power input to the ice thus drops to $\sim 2 \frac{\text{mwatt}}{\text{m}^2}$ with an extreme value of $\sim 100 \frac{\text{mwatt}}{\text{m}^2}$. When the ice is motionless of course no energy is transferred to it and all of the energy in the PBL is dissipated.

The energy transferred to currents will be very similar to the values for the ice in summer. The drag coefficient over water varies with the sea surface state. Kraus (1972) gives $C_{10} \sim 1.3 \times 10^{-3}$ which means that the power transfer coefficients are ~.65 times the values given for ice in the summer. The power input to the currents per unit area will not vary much with time of year. The total power within a unit grid available to drive currents will be affected most by the amount of open water available. In open water, of course, all the power goes into the water. In the Arctic summertime there is typically only 10% open water overall, but large open areas of water appear occasionally.

In winter much less open water is available to transfer energy from winds directly to currents. Furthermore ice motions are restricted in the winter so that the ice transfers less energy to currents. In summer free drift ice motions should transfer a considerable part of their energy to the oceanic mixed layer. The bulk of this energy will be dissipated in the OML as turbulence, but some will be transferred to currents by the work of Reynolds stresses. When the ice moves with a current no work is done since the Reynolds stress is zero. When the current is zero or at 90° to the ice motion no work is done either and all the kinetic energy is lost to turbulence. Energy transfer occurs

-30-

when the ice and current have velocity components which are parallel but different. Energy may be transferred from ice to currents and vice versa.

Typical ice velocities with respect to currents are 1 to 14 cm/s. A 1m water drag coefficient has been estimated by Langleben (1980) as $C_1 = 4.1 \times 10^{-3}$. The shear stress is

$$\tau_w = \rho_w C_1 u_1^2 \quad (7.15)$$

where u_1 is the relative current velocity 1 m beneath the ice. The energy transferred into or out of the ice will be

$$P_{i,c} = \pm \tau_w u_1 \quad (7.16)$$

or

$$P_{i,c} = \pm \rho_w C_1 u_1^3 \quad (7.17)$$

u_1 is typically between 1 and 10 cm/s giving a transfer power of 0.004 to 4 mwatt/m².

The energy input to the ice has been estimated at 5 to 300 mwatt/m². The difference between this value and the power transferred to the OML must be taken up by ice deformation. Pritchard (1981) has estimated the rates of energy dissipation by ice deformation at 0 to 200 mwatt/m² by using the full AIDJEX model. Almost all of this power could be transferred from one area to another via the stress flux. The rate of working by winds upon a fully developed sea is, (Kraus, 1972)

$$W \sim .05 u_{10} \tau \quad (7.18)$$

where τ is the Reynolds stress $\tau = \rho_a C_{10} u_{10}^2$ with $C_{10} = 1.3 \times 10^{-3}$.

The rate of working is a maximum in a fully developed sea since wave velocities and surface roughness are maximized. In the Arctic the fetch is rarely large enough to generate such a sea state and in fact fully developed seas are found only occasionally in the open ocean. The

rate of working on intermediate sea states is not known or even estimated but must be less than the maximum value given. The maximum for a typical wind of 5 m/s is about

$$W_{\max} \sim 10 \frac{m \text{ watt}}{m^2} \quad (7.19)$$

If the wind reaches an extreme value of 20 m/s this power can increase drastically to

$$W_{\max} \sim 700 \frac{m \text{ watt}}{m^2} \quad (7.20)$$

Arbitrarily assuming half the power for an intermediate sea state gives rates of working on waves roughly equivalent to the rates on ice or currents.

8. Discussion

Mechanical energy flow charts for a variety of Arctic conditions are shown in Figure 4. Four geographic locations are shown. For two of these, Central Arctic Basin (CAB) and Shear Zone, conditions are significantly different in summer and winter and these are shown.

The flow of mechanical energy into the open ocean is considered first as a reference point. In the Arctic summer and winter atmospheric energy levels are not significantly different, so only one flow chart is shown. The mechanical energy of the PBL is mostly dissipated by turbulence. The remainder is shown to be split evenly between waves and the OML. These power levels are somewhat arbitrary since it is difficult to separate the direct driving of the OML from that mediated by waves. Much of the wave energy is lost due to wave breaking. Some is transferred to the OML currents and a considerable amount can be radiated out of the area. This is the major source for long wavelength wave energy in the marginal ice zone (MIZ). Only in open water is the fetch sufficient to generate significant wave energy.

The mechanical energy flow in the marginal ice zone is considerably more complex. Assuming 50 % ice in this region means that about half the available energy from the PBL drives the ice directly. Ice mechanical

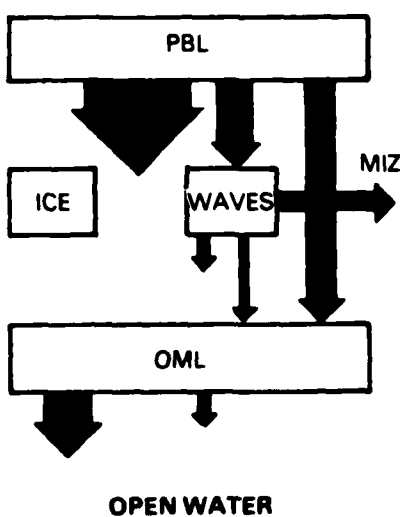
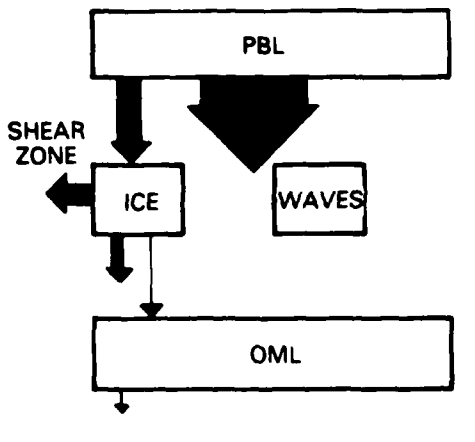
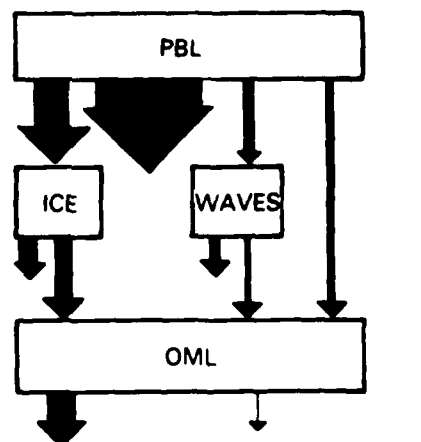
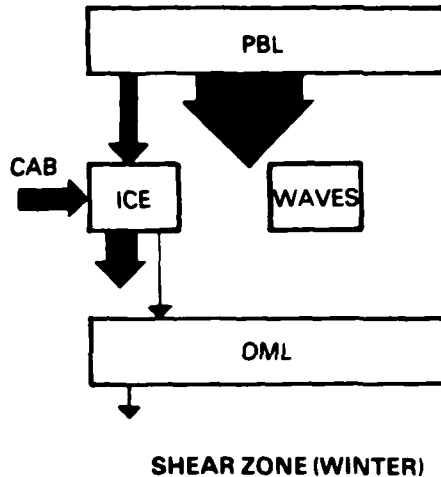
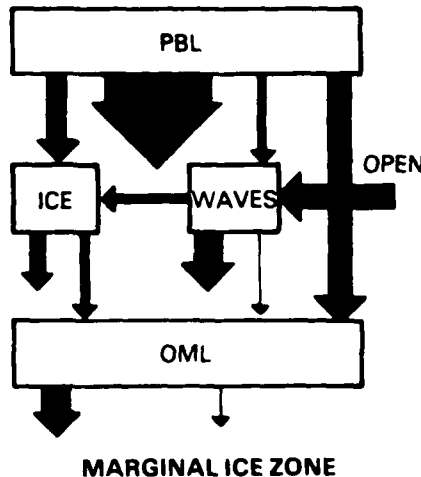


Figure 4. Mechanical Energy Flow Patterns Under Various Arctic Conditions. Logarithmic Magnitudes of Transfer Terms are Roughly Indicated by the Sizes of the Arrows Refer to Figure 3 to Identify Terms.

-33-

energy can be dissipated by floe bumping and grinding and by Reynolds stresses in the OML. The interaction of swells with the ice can also be significant near the ice margin. The source of wave swell energy in the MIZ is swells generated outside the area. Short wave lengths may be generated within the MIZ. Their interaction with the OML will be the same as in open water. The presence of ice will severely limit wave generation by dissipating wave energy in breaking against ice flows.

The ice completely dominates energy flow in the CAB. Only 1-2% open water exists here in winter, so all the mechanical energy available from the PBL moves into the ice. The ice moves more slowly than open water currents so the energy transferred is low. Furthermore, ice deformation tends to concentrate near shorelines so energy dissipation should be low. The energy transferred to the ice will be transmitted by stress flux to other regions especially the Shear Zone. A small amount of energy will be transferred to the OML by the ice motions.

In the summer as much as 10% open water is found in the CAB. Energy transfers power to waves and OML currents are thus shown to be about 10% of that input to the ice. The open water also reduces the strength of the ice to zero thus essentially no mechanical energy is transmitted to the Shear Zone in summer. The ice moves more in summer so more energy is transferred to it. A considerable amount of this energy is lost by deformation at flow boundaries in the summer. Therefore, less energy is left to transfer into the OML than in open water. This is why Arctic Ocean currents are considerably less energetic than their mid-latitude counterparts.

Only one flow chart is shown for the Shear Zone in winter. In the summer the mechanical energy flow is essentially the same as in the CAB. In winter the only difference is the mechanical transmitted into the Shear Zone from the CAB. This causes a large increase in the dissipation of energy by ridging and other forms of deformation in this region.

9. Conclusion

Mechanical energy balance equations have been written for the various "layers" important to the transfer of energy from the atmosphere into an ice covered ocean. These equations are coupled by the transfer of energy from one into another. This coupling is presented graphically in the form of a mechanical energy flow chart. The magnitudes of the transfer terms have been estimated and presented in flow chart form for a variety of Arctic conditions.

The presence of a sea ice cover has been shown to have a profound effect on the flow of mechanical energy into the Arctic Ocean. In both summer and winter the energy available to drive currents is severely restricted. Instead, this energy goes into deforming the ice pack. Most of the deformation is concentrated in a Shear Zone. The levels of power being dissipated have been estimated.

The interaction of waves with ice has also been considered. The presence of ice provides an important means for dissipating wave energy by wave breaking. Long period swells generated in the open ocean dissipate their energy quickly at the ice margin. The levels of power transfer indicate that this may be an important noise generation region.

Appendix

Typical and extreme values for currents, ice motions, winds, and ice cover in the Beaufort Sea.

A) Currents

Mixed layer currents to ~ 30 m. Mean surface drift velocities averaged over 20 days during AIDJEX Pilot project were 2 cm/s to the southwest over the CAB (Hunkins, 1974).

Currents in the off-shore region may be considerably higher typically 5 cm/s for the prevailing currents to 50 cm/s around points or driving storms in open water (Brower, et al., 1977).

Fluctuating parts of currents are larger than the mean typically 10 cm/s in CAB with extreme to 14 cm/s under ice turbulent kinetic energy at 7 ergs/cm³ (Hunkins, 1974). McPhee (1980) equates free drift of ice with mixed layer current in summer ice drifts at 0-25 cm/s. Wiseman (1974) has observed surface currents averaging 14 cm/s with extremes to 34 cm/s in open water, offshore, driven by winds. Surface currents under fast ice in shallow water are very small 5 cm/s (Anguard, 1980).

Sub-surface flow ~ 50 to 300 m depth. Mean flow ~ same as surface drift maybe a little less ~ 2 cm/s (Hunkins, 1974). Fluctuations flow - baroclinic eddies velocity maximum at ~ 150 m at 40 cm/s or more is often observed. Kinetic energy at this level is 63 erg/cm³ (Hunkins, 1974, 1980).

B) Winds

Geostrophic calculations gives synoptic free stream flow above the planetary boundary layer averages ~ 9 m/s both summer and winter.

Surface winds due to geostrophic winds average ~ 5 m/s summer and winter (Albright, 1980). Extreme surface winds of 20 m/s are observed. (Brower et al., 1977). Mean of vector winds over days 105-180 is 71 cm/s at 065°.

C) Ice Motions AIDJEX 1972, 1975-6

Mean Drift (summer) mean drift is ~ 2.4 cm/s (Hunkins, 1974) in the same direction as the geostrophic current.

Fluctuating ice speeds are ~ 10 cm/s with extremes to 36 cm/s in summer and less in winter ~ 1 cm/s with extremes to ~ 20 cm/s in the CAB. One station moved 140 cm/s through highly fractured ice. (Thorndike and Colony, 1980).

Mean drift in winter is about the same ~ 2 cm/day. Fluctuations in winter are less ~ 1 cm/s with extremes to 20 cm/s (Thorndike and Colony, 1980).

Near shore ice is essentially motionless all winter.

D) Ice cover (Weeks, 1976)

		Mean	Range
<u>Offshore</u>	Summer	78%	8 - 100%
	Winter	99%	70 - 100%
<u>CAB</u>	Summer	92%	30 - 100%
	Winter	99%	98 - 100%

E) Ice Thickness Distribution (topography)

Yearly average from Blidberg (1979) of all AIDJEX data gives an average thickness $\bar{h} = 426$ cm.

In winter Swithinbank's (1971) and Le Schack's (1972) thickness distributions give an average of $\bar{h} = 628$ cm.

In August 1963 Thorndike et al., (1974) estimate an average thickness distribution of $\bar{h} = 350$ cm.

F) Dissipation of energy by ice deformation in winter = $\epsilon_I \dot{\epsilon}_I + \epsilon_{II} \dot{\epsilon}_{II}$
also depends on strength (Table 1) and location since deformation is localized $0 - 20 \frac{\text{m watt}}{\text{m}^2}$ in middle of pack to $20 - 100 \frac{\text{m watt}}{\text{m}^2}$ in boundary shear zone (Pritchard, 1981).

In summer more than 10% (usually 10 - 30 %) of the pack is open water, though strains may be large the stresses are small. Energy dissipation may occur through uncorrelated high frequency motions causing collisions between ice sheets. Motions between the AIDJEX stations BB and SB are essentially uncorrelated at frequencies above 1/8 per hour and have mean velocities of ~ .5 cm/s (Colony, 1980 unpub.) from spectral density plot. A flow grinding against another could cause an appreciable release of energy locally. The strength of pack ice in summer has been shown to be negligible, however, so that the energy released overall by this mechanism should be negligible as well.

Table 1. Crushing and Buckling Strengths from Rothrock (1980)

Ice Thickness n	Crushing Stress 10^5 N/m	Buckling Stress 10^5 N/m	Ridging Stress 10^5 N/m
0.10	0.3	0.2	0.0017
0.50	4.5	2.7	0.042
1.00	15.0	8.7	0.17
3.00	60.0	50.0	1.5

G) Drag Coefficients

Ice-water drag coefficient for 1m reference velocity

$$C_1 = 4.14 \times 10^{-3} \quad (\text{Langleben, 1980})$$

Stress is given by

$$|\tau_w| = \rho_w C_1 u_1^2$$

where u_1 is current velocity at 1 m below ice, ρ_w = density of water.

Air-ice drag coefficient for 10m wind velocity $C_{10} = 1.58 \times 10^{-3}$ (Banke et al., 1980) for pack ice free of major ridges. Leavitt (1980) gives $C_{10} \sim 2 \times 10^{-3}$.

Air-sea drag coefficient depends on sea state. Kraus (1972) gives $C_{10} = 1.3 \times 10^{-3}$.

References

Aagard, K. and D. Haugen, "Current Measurements in Possible Dispersal Regions at the Beaufort Sea," annual report, in Environmental Assessment of the Alaskan Continental Shelf, OCSEAP, 1980.

Albright, M., "Geostrophic Wind Calculations for AIDJEX," in Sea Ice Processes and Models, edited by R. S. Pritchard, 402-418, University of Washington Press, Seattle, 1980.

Banke, E. G., S. D. Smith and R. J. Anderson, "Drag Coefficients at AIDJEX from Sonic Anemometer Measurements," in Sea Ice Processes and Models, edited by R. S. Pritchard, 430-442, University of Washington Press, Seattle, 1980.

Blidberg, D. R., R. W. Corell and A. S. Westnent, "Probable Ice Thickness of the Arctic Ocean," POAC 1979, Vol. 1, University of Trondheim, p. 253-267, 1979.

Brown, R. A., "Planetary Boundary Layer Modeling for AIDJEX," in Sea Ice Processes and Models, edited by R. S. Pritchard, 387-401, University of Washington Press, Seattle, 1980.

Callaway, R. J. and C. Koblinsky, "Transport of Pollutants in the Vicinity of Prudhoe Bay, Alaska," OCSEAP 76, Vol. 2 Ru 335, p. 427-755, 1976.

Carsey, F. D., "The Boundary Layer in Air Stress Measurement," in Sea Ice Processes and Models, edited by R. S. Pritchard, p. 443-451, University of Washington Press, Seattle, 1980.

Coantic, M. F., "An Introduction to Turbulence in Geophysics, and Air-Sea Interactions," Lecture Notes, A.M.E.S. 2226 Spring 1975, University of California, San Diego, p. 283, 1975.

Coon, M. D. and R. S. Pritchard, "Mechanical Energy Considerations in Sea Ice Dynamics," Jour. Glaciology, p. 94, 1979.

Holland, W. R. and L. B. Lin, "On the Generation of Mesoscale Eddies and their Contribution to the Oceanic General Circulation, I. A preliminary numerical experiment. II. A parameter study," J. Phys. Oceanogr., 5, 642-657 (I), 658-669 (II), 1975.

Hunkins, K. L., "Subsurface Eddies in the Arctic Ocean," Deep-Sea Res., p. 21, 1017-1033, 1974.

Hunkinss, K., "Review of the AIDJEX Oceanographic Program," in Sea Ice Processes and Models, edited by R. S. Pritchard, p. 34-45, University of Washington Press, Seattle, 1980.

Kinsman, B., "Wind Waves," Prentice-Hall, N. J., p. 676, 1965.

Kraus, E. B., "Atmosphere Ocean Interaction," Clarendon Press, Oxford, 1972.

Langleben, M. P., "Water Drag Coefficient at AIDJEX, Station Caribou," in Sea Ice Processes and Models, edited by R. S. Pritchard, p. 464-471, University of Washington Press, Seattle, 1980.

Lavrov, V. V., "Deformation and Strength of Ice," Gidrometeorologicheskoe Izdatel'stvo, (English translation by Iseael Prog. for Sci. Trans., Jerusalem), 1969.

Leavitt, E., "Surface Based Air Stress Measurements Made During AIDJEX," in Sea Ice Processes and Models, edited by R. S. Pritchard, p. 419-429, University of Washington Press, Seattle, 1980.

Lumley, J. L., and H. A. Panofsky, "The Structure of Atmospheric Turbulence," Interscience, New York, 1964.

McPhee, M. G., "An Analysis of Pack Ice Drift in Summer," in Sea Ice Processes and Models, edited by R. S. Pritchard, p. 62-75, University of Washington Press, Seattle, 1980.

Newton, J. L., "The Canada Basin: Mean Circulation and Intermediate Scale Flow Features," PhD. dissertation, University of Washington, Seattle, Washington, 1973.

Phillips, O. M., "The Dynamics of the Upper Ocean," University Press, Cambridge, 1966.

Phillips, O. M., "The Dynamics of the Upper Ocean, Second Edition," University Press, Cambridge p. 336, 1977.

Pritchard, R. S., "Mechanical Behaviour of Pack Ice," in Mechanical Behavior of Structured Media, edited by A.P.S. Selvadurai, Elsevier, Amsterdam, 1981.

Robin, G. de Q., "Wave Propagation through Fields of Pack Ice," Phil. Trans. Roy. Soc. London, Ser A, 225, 313-339, 1963.

Roll, H. U., "Physics of the Marine Atmosphere," Academic Press, New York, 1965.

Rothrock, D. A., "Modeling Sea-Ice Features and Processes," Jour. Glaci., 24, 359-376, 1980.

Thorndike, A. S., D. A. Rothrock, G. A. Maykut, and R. Colony, "The Thickness Distribution of Sea Ice," Jour. Geophys. Res., 80, 4501-4513, 1975.

Thorndike, A. S. and R. Colony, "Large Scale Ice Motion in the Beaufort Sea during AIDJEX," in Sea Ice Processes and Models, edited by R. S. Pritchard, 249-260, University of Washington Press, Seattle, 1980.

Wadhams, P., "Attenuation of Swell by Sea Ice," J. Geophys. Res., 78, 3552-3563, 1973.

Weeks, W. F., "Sea Ice Conditions in the Arctic," AIDJEX Bull., 34, 173-196, 1976.

Wiseman, W. S., J. N. Suhayda, S. A. Hsu, and C. D. Walters, "Characteristics of Nearshore Oceanographic Environment of Arctic Alaska," in The Coast and Shelf of the Beaufort Sea, edited by J. C. Reed and J. E. Suter, The Arctic Institute of North America, Arlington, 49-69, 1974.

